A phononic rectifier based on carbon schwarzite host-guest system

Zhongwei Zhang(张忠卫), Yulou Ouyang(欧阳宇楼), Jie Chen(陈杰), and Sebastian Volz
Citation: Chin. Phys. B, 2020, 29 (**12**): 124402. DOI: 10.1088/1674-1056/abbbf9
Journal homepage: http://cpb.iphy.ac.cn; http://iopscience.iop.org/cpb

What follows is a list of articles you may be interested in

A phononic rectifier based on carbon schwarzite host-guest system

Zhongwei Zhang(张忠卫), Yulou Ouyang(欧阳宇楼), Jie Chen(陈杰), and Sebastian Volz
Chin. Phys. B, 2020, 29 (**12**): 124402. DOI: 10.1088/1674-1056/abbbf9

Scaling behavior of thermal conductivity in single-crystalline α-Fe_2O_3 nanowires

Qilang Wang(王啟浪), Yunyu Chen(陈允玉), Adili Aiyiti(阿地力·艾依提), Minrui Zheng(郑敏锐), Nianbei Li(李念北), Xiangfan Xu(徐象繁)
Chin. Phys. B, 2020, 29 (**8**): 084402. DOI: 10.1088/1674-1056/ab90f0

Polarization resolved analysis of phonon transport in a multi-terminal system

Yun-Feng Gu(顾云风), Liu-Tong Zhu(朱留通), Xiao-Li Wu(吴晓莉)
Chin. Phys. B, 2019, 28 (**12**): 124401. DOI: 10.1088/1674-1056/ab4d3e

General theories and features of interfacial thermal transport

Hangbo Zhou(周杭波), Gang Zhang(张刚)
Chin. Phys. B, 2018, 27 (**3**): 034401. DOI: 10.1088/1674-1056/27/3/034401

Reversal of thermal rectification in one-dimensional nonlinear composite system

Zhan Si-Qi, Huang Wei-Qing, Huang Gui-Fang
Chin. Phys. B, 2014, 23 (**11**): 114401. DOI: 10.1088/1674-1056/23/11/114401

SPECIAL TOPIC — Phononics and phonon engineering

A phononic rectifier based on carbon schwarzite host–guest system*

Zhongwei Zhang(张忠卫)[1,2,3], Yulou Ouyang(欧阳宇楼)[1,2], Jie Chen(陈杰)[1,2,†], and Sebastian Volz[2,4,‡]

[1] Center for Phononics and Thermal Energy Science, School of Physics Science and Engineering, Tongji University, Shanghai 200092, China
[2] China-EU Joint Laboratory for Nanophononics, Tongji University, Shanghai 200092, China
[3] Institute of Industrial Science, The University of Tokyo, Tokyo 153-8505, Japan
[4] Laboratory for Integrated Micro and Mechatronic Systems, CNRS-IIS UMI 2820, The University of Tokyo, Tokyo 153-8505, Japan

(Received 28 July 2020; revised manuscript received 23 September 2020; accepted manuscript online 28 September 2020)

Thermal rectification is a promising way to manipulate the heat flow, in which thermal phonons are spectrally and collectively controlled. As phononic devices are mostly relying on monochromatic phonons, in this work we propose a phononic rectifier based on the carbon schwarzite host–guest system. By using molecular dynamic simulations, we demonstrate that the phononic rectification only happens at a specific frequency of the hybridized mode for the host–guest system, due to its strong confinement effect. Moreover, a significant rectification efficiency, $\sim$ 134 %, is observed, which is larger than most of the previously observed efficiencies. The study of length and temperature effects on the phononic rectification shows that the monochromaticity and frequency of the rectified thermal phonons depend on the intrinsic anharmonicity of the host–guest system and that the on-center rattling configuration with weak anharmonicity is preferable. Our study provides a new perspective on the rectification of thermal phonons, which would be important for controlling monochromatic thermal phonons in phononic devices.

Keywords: thermal rectification, phonon, thermal transport

PACS: 44.10.+i, 66.70.+f, 05.45.−a, 63.20.−e **DOI:** 10.1088/1674-1056/abbbf9

1. Introduction

Thermal rectification, which manipulates the propagating of heat flow, attracted a lot of research attention in the past decades.[1–3] In 2004, Li *et al.*[4] demonstrated thermal rectification in asymmetric atomic chains. After that, many experimental and theoretical explorations of thermal rectification were performed in nanomaterials,[5–15] in which researchers mostly focused on improving the rectification efficiency to promote its realistic application. For example, Hu *et al.*[13] proposed a series circuit concept for thermal rectifiers to enhance the thermal rectification. Recently, Jiang *et al.*[15] found by engineering the thermal contacts that the rectification ratio of graphene nanoribbon can reaches 920%, even for the symmetric structure.

Because of the collective excitation of the thermal phonons,[16,17] the controlled heat flow in thermal rectifiers is spectrally distributed.[11,14] However, phonons are also demonstrated as new carriers to control and exchange information in phononic related fields,[18–21] such as phonon counting, quantum communication, etc., in which the monochromatic phonons, i.e., with a set frequency, are demanded.[22,23] Due to the complexity of thermal excitation, the control of monochromatic phonons in phononic devices has been rarely reported before. The study of phononic rectifiers that allow for the manipulation of the directional propagation of specific frequency phonons but without affecting phonons at other frequencies is meaningful for the phononic related fields.

Recently, host–guest systems, such as clathrates, perovskites, and skutterudites,[24–27] were demonstrated to be a platform to manipulate phonons.[23,28,29] Due to the weak interaction with the host cages, the guest atoms in a host-guest system (HGS) exhibits an isolated rattling behavior, which further results in the hybridized phonon modes. The zero group velocity makes a strong phonon confinement of the hybridized modes in HGS.[30,31] As an inherent feature of HGSs, the unique phonon confinement of the hybridized mode provides a novel tool to control monochromatic phonons. Because of the large void space, Zhang *et al.*[23,29] found that carbon schwarzite is a promising base to construct the host–guest system by inserting guest atoms, in which the hybridized mode almost exhibits monochromatic frequency. In addition, the external strain and the replacement of guest atoms are demonstrated as effective ways to regulate the frequency of the hybridized mode in the carbon schwarzite host–guest system.[23,29,30] These features make it an ideal case to control phonons at nanoscale.

*Project supported in part by the National Natural Science Foundation of China (Grant No. 11890703), Science and Technology Commission of Shanghai Municipality, China (Grant Nos. 19ZR1478600 and 18JC1410900), and the Fundamental Research Funds for the Central Universities, China (Grant No. 22120200069). This work was partially supported by CREST JST (Grant Nos. JPMJCR19Q3 and JPMJCR19I1). Z. Z. gratefully acknowledges financial support from China Scholarship Council.

†Corresponding author. E-mail: jie@tongji.edu.cn
‡Corresponding author. E-mail: volz@iis.u-tokyo.ac.jp

In this work, based on the carbon schwarzite[29,32–34] host–guest system, we propose a phononic rectifier. By using molecular dynamic (MD) simulation, we study the spectral rectification of thermal phonons for this phononic rectifier. Compared to the thermal rectification of full spectrum heat flux in previous reports,[5–7,9–15] the proposed phononic rectifier exhibits the rectification phenomenon for a specific frequency, while the rectification at other frequencies vanishes. Then, the length and temperature effects on the phononic rectification are also discussed. Our study provides a new understanding of thermal rectification and a pathway to control monochromatic thermal phonons.

2. Model and methodology

The atomic structure of the asymmetric phononic rectifier is shown in Fig. 1, which is composed of two homogeneous parts: the HGS layers at the left side and the schwarzite cage at the right side. The primitive cells of the two segments are displayed in the upper plane of Fig. 1. The carbon schwarzite structure is obtained from Refs. [33,35], having a large void space to insert atoms. By inserting the Fe atoms to the schwarzite cages, we build up the schwarzite HGS cell, as shown in the left inset of Fig. 1. The total length along x direction of the phononic rectifier is L, and the length of the left HGS is L_0. While, y and z are the directions along cross-section with width W. In this work, L and W are respectively fixed at 319.3 nm and 3.9 nm. To establish the temperature gradient, the two ends of the phononic rectifier are coupled to the heat baths, respectively with temperatures $T_{\rm hot}$ and $T_{\rm cold}$.

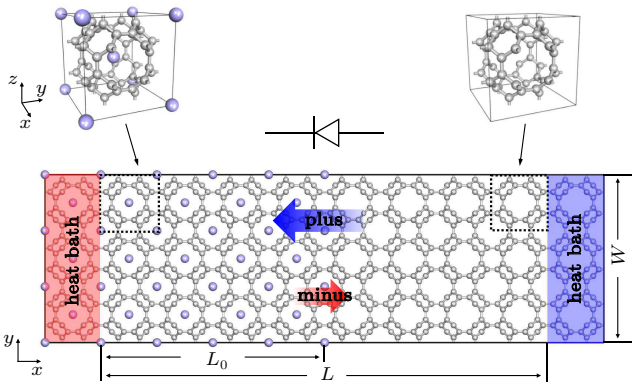

Fig. 1. Schematic figure of the phononic rectifier. Atomistic structure for the phononic rectifier composed of HGS at the left side and the carbon schwarzite at the right side. To establish the temperature difference, at both ends, the phononic rectifier is coupled to heat baths. The gray and blue atoms are C atoms in the schwarzite cage and guest Fe atoms, respectively. The upper plane figures show the perspective views of the primitive cell for the two segments. The dimensions of the rectifier are labeled as L and W, and the length of HGS is L_0.

We use classical MD simulations to study the rectification of thermal phonons. The covalent C–C interaction in the schwarzite cage is modeled by the optimized Tersoff potential,[36] and the non-bonded interaction between the schwarzite cage and guest Fe atoms is modeled by the Lennard–Jones (LJ) potential with LJ parameters $\varepsilon = 1.59$ meV and $\sigma = 3.01$ Å from universal force field.[37] Our previous study[29] showed that the LJ potential can well describe the weak interactions between the cages and Fe guest atoms. Periodic boundary condition is applied along the y and z directions. To control the temperature of the heat baths, the Nosé–Hoover thermostat[38] is applied. All MD simulations are performed by using the LAMMPS package[39] with a timestep of 0.35 fs. Firstly, the system runs 1×10^7 steps to establish the non-equilibrium steady state. Then, the simulation runs over 5×10^6 steps to study the thermal transport.

3. Temperature distribution

3.1. Nonlinear temperature distribution

To study the thermal rectification along the rectifier, two directional temperature gradients are applied. As shown in Fig. 2(a), the plus indicates the heat energy transfer from the right (schwarzite) to the left (HGS) side, while the reversed direction is labeled by a minus sign (see Fig. 1). With the temperatures $T_{\rm hot} = 500$ K and $T_{\rm cold} = 100$ K, the steady state temperature distribution of $L_0/L = 0.05$ system is shown in Fig. 2(a). Compared to the linear distribution of temperature in symmetric homogeneous materials,[40,41] a nonlinear temperature distribution is observed in our calculation, which agrees well with other reports about thermal rectifiers.[9,13] There is even a temperature jump across the interface of the inhomogeneous rectifiers.[4,10] The nonlinear temperature distribution results from the asymmetric thermal resistance along the rectifier. This asymmetry is also responsible for the thermal rectification in nanomaterials. Due to the limited difference between HGS and schwarzite cage (see detailed discussion in the next section), in our phononic rectifier, the nonlinear distribution or interfacial temperature change between HGS and schwarzite is not as significant as that in other thermal rectifiers presented in other reports.[9,13] Correspondingly, the overall heat flux rectification efficiency is only 3.2 % (not shown).

3.2. Temperature dependent hybridized mode in HGS

However, due to the isolated rattling of the guest atoms, the HGS and schwarzite should have distinct modal behaviors around the frequency of the hybridized modes. To gain insight into the modal phonon information, we perform the spectral energy density (SED) analysis. The phonon energy at wavevector $\boldsymbol{k}$ and frequency ω, $E(\boldsymbol{k},\omega)$, can be calculated by the Fourier transform of phonon normal mode velocity $\dot{q}\left(\begin{matrix}\boldsymbol{k}\\ b\end{matrix};t\right)$,[42,43]

$$E(\boldsymbol{k},\omega) = \frac{1}{4\pi t_0 N}\lim_{t_0\to\infty}\sum_{b}^{n_b}\left|\int_0^{t_0}\dot{q}\left(\begin{matrix}\boldsymbol{k}\\ b\end{matrix};t\right)\mathrm{e}^{-\mathrm{i}\omega t}\,\mathrm{d}t\right|^2, \quad (1)$$

where N is the number of cells, N_b is the number of atoms in one unit cell, and t_0 is the simulation time. The phonon normal mode velocity $\dot{q}\begin{pmatrix}\boldsymbol{k}\\ b\end{pmatrix};t\Big)$ is defined by

$$\dot{q}\left(\begin{matrix}\boldsymbol{k}\\ b\end{matrix};t\right)=\sum_{l}^{N}\sqrt{\frac{m_b}{N}}\boldsymbol{v}_{bl}\left(t\right)\mathrm{e}^{\mathrm{i}\boldsymbol{k}\cdot\boldsymbol{R}_{0l}}, \tag{2}$$

where m_b is the mass of the b-th atom in the unit cell, $\boldsymbol{v}_{bl}\left(t\right)$ is the velocity of the b-th atom in the l-th unit cell at time t, and $\boldsymbol{R}_{0l}$ is the equilibrium position of the l-th unit cell.

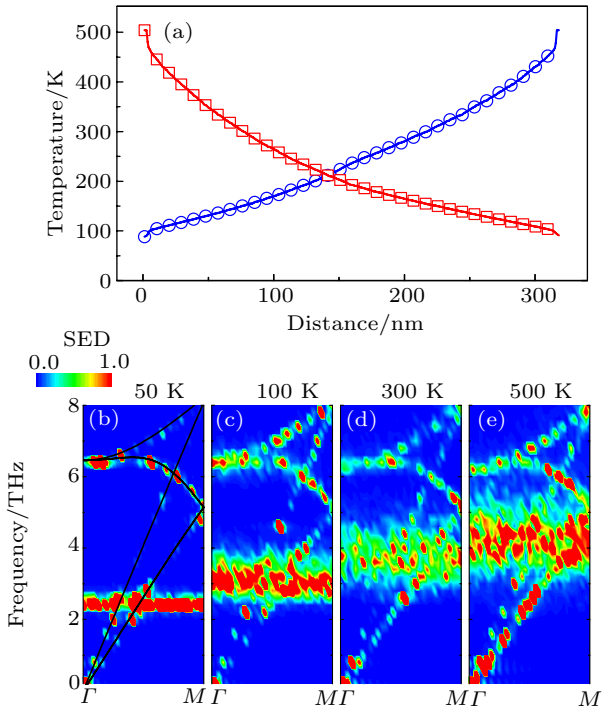

Fig. 2. Temperature distribution and its effect in the phononic rectifier. (a) Temperature distribution along x direction of the phononic rectifier for plus and minus transport directions. The system is computed with $L_0/L=0.05$, and temperatures are fixed to $T_{\mathrm{hot}}=500$ K and $T_{\mathrm{cold}}=100$ K. Temperature dependent spectral energy density (SED) of HGS at (b) 50 K, (c) 100 K, (d) 300 K, and (e) 500 K. The black line in (b) is the phonon dispersion of pure carbon schwarzite from lattice dynamic calculations.

The calculated SED spectra for the HGS system at temperatures 50 K, 100 K, 300 K, and 500 K are shown in Figs. 2(b)–2(e). Compared to the pure carbon schwarzite structure, there is an additional hybridized mode (ω_{h}) appearing in the low frequency region as a flat band (see Fig. 2(b)). The flat hybridized mode results from the weak interaction between the guest atoms (Fe) and host cages (carbon schwarzite). The zero group velocity of the hybridized modes further leads to the confinement of phonons around ω_{h}. The confinement at ω_{h} makes the control of monochromatic phonons in the phononic rectifier possible.

Moreover, because of the anharmonicity of HGS, the frequency of ω_{h} and also its broadening strongly depend on the temperature. When increasing temperature, ω_{h} is shifted to the high frequency region and the linewidth becomes broader, as shown in Figs. 2(b)–2(e). Therefore, as a longer HGS segment (L_0) is integrated in the phononic rectifier, a broader range of frequency of phonons are confined in the system. L_0 should be a critical factor to realize the phononic rectifier.

4. Phononic rectification

4.1. Rectification efficiency

To further study the propagating of thermal phonons in the rectifier, the spectral heat flux along plus/minus directions, i.e., $Q_{\mathrm{p/m}}\left(\omega\right)$, across the interface can be defined as[44,45]

$$Q_{\mathrm{p/m}}\left(\omega\right)=\frac{2}{A}\mathrm{Re}\sum_{j\in H}\sum_{i\in C}\int_{\infty}^{-\infty}\left\langle \boldsymbol{F}_{ij}\left(t\right)\cdot\boldsymbol{v}_i\left(t\right)\right\rangle \mathrm{e}^{\mathrm{i}\omega t}\,\mathrm{d}t, \tag{3}$$

where i and j are the atoms in the cold region (C) and hot region (H) at the two sides of the interface, A is the interface area, $\boldsymbol{F}_{ij}$ is the pair force between the i-th and j-th atoms across the interface, and $\boldsymbol{v}_i$ is the atomic velocity in the cold temperature side. Moreover, to obtain the output spectral heat flux of the phononic rectifier, the interface is set at the last two unit cells in the cold temperature region, which means that we change the location when reversing the temperature gradient.

Figure 3(a) shows $Q_{\mathrm{p/m}}\left(\omega\right)$ calculated for the system with $L_0/L=0.05$, $T_{\mathrm{hot}}=500$ K, and $T_{\mathrm{cold}}=100$ K. There is a difference between $Q_{\mathrm{p/m}}\left(\omega\right)$ appearing at 3.4 THz. The frequency is close to the ω_{h} of HGS at 100 K, i.e., the temperature of T_{cold}. Obviously, the difference in $Q_{\mathrm{p/m}}\left(\omega\right)$ results from the phonon mode blocking by the flat hybridized band in HGS. Moreover, the $Q_{\mathrm{p/m}}\left(\omega\right)$ is mainly determined by the phonon information in the cold ouput side.

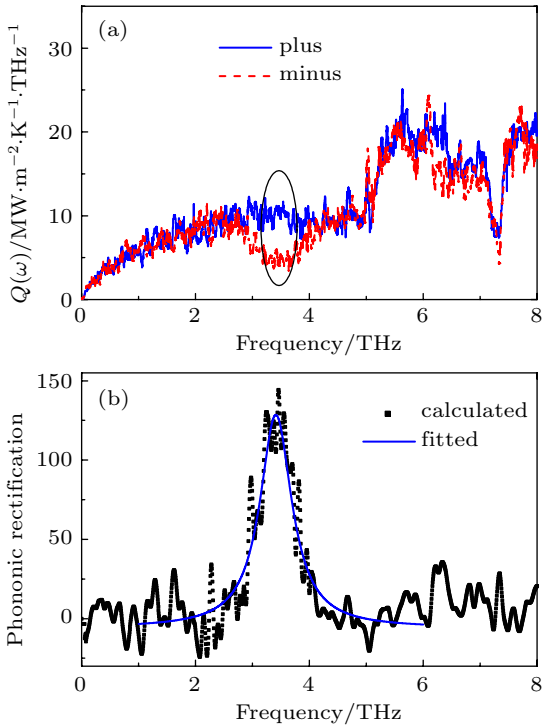

Fig. 3. The rectification in the phononic rectifier. (a) Spectral heat flux $Q_{\mathrm{p/m}}\left(\omega\right)$ in the phononic rectifier. (b) Phononic efficiency in phononic rectifier. The dots are calculated from MD results, and the solid blue line is fitted by the Lorentzian function. The size of the system is $L_0/L=0.05$, and the temperatures are fixed at $T_{\mathrm{hot}}=500$ K and $T_{\mathrm{cold}}=100$ K.

As demonstrated before, the asymmetric heat flux is the origin of thermal rectification in nanostructures.[6,9,11] Accordingly, the asymmetric spectral heat flux in Fig. 3(a) would result in the rectification phenomenon of thermal phonons. The phononic rectification efficiency is defined as

$$R(\omega) = \frac{|Q_{\rm p}(\omega) - Q_{\rm m}(\omega)|}{Q_{\rm m}(\omega)} \times 100\%. \quad (4)$$

The obtained phononic rectification efficiency of the $L_0/L = 0.05$ system is displayed in Fig. 3(b). There is a peak emerging at 3.4 THz, which agrees well with the difference in spectral heat fluxes in Fig. 3(a). The peak demonstrates the happening of phononic rectification around 3.4 THz. To clarify its monochromaticity, we further use the Lorentzian function to fit the spectral rectification spectrum. As shown by the solid blue line in Fig. 3(b), the modeling results can be well fitted, indicating the control of monochromaticity of phonons in the phononic rectifier. Moreover, the rectification efficiency at $\omega_{\rm h}$ reaches 134%, which is larger than most of the previously reported rectification efficiencies in nanostructures.[6,9,11–14]

It should be noted that the broadening of the phononic rectification depends on the anharmonicity of the HGS. As the HGS has strong anharmonicity, the broadening of the hybridized modes in the HGS is increased and then the monochromaticity is suppressed in the rectifier. Previous studies showed that this effect can be tuned by introducing different guest atoms to the cage, as the anharmonicity is accordingly changed.[23,29] On the other side, the reduced anharmonicity would also enhance the rectification efficiency at $\omega_{\rm h}$, as the phonons of $\omega_{\rm h}$ mode are less scattered and highly confined.

4.2. Length effect

As we discussed in Fig. 2, the temperature gradient distribution and length of HGS makes the HGS cells take different temperatures, and the $\omega_{\rm h}$ is shifted to different frequencies due to the anharmonicity of HGS. This phenomenon was also reported before in HGS, especially for the off-center rattling case.[29] Thus, the rectification efficiency should depend on the length of HGS, as shown in Fig. 4. When the HGS has longer length in the rectifier, more phonon modes are blocked because of the frequency shifting (see Fig. 2). Accordingly, the phononic rectification of monochromatic phonons is failing. Only as the HGS length is decreasing to small value, for instance $L_0/L = 0.05$ in Fig. 4, only one peak in rectification appears, indicating the success of phononic rectification to control monochromaticity of thermal phonons. Moreover, compared to the system of $L_0/L = 0.05$, a longer rectifier blocks more phonon modes in a wider spectrum. Although blocking a wider phonon range leads to the failure of monochromatic phononic rectification, it significantly improves the rectification of heat flux. The calculations show that the thermal rectification efficiency of heat flux is enhanced by 4.1 and 4.7 times as L_0/L increases from 0.05 to 0.1 and 0.5, respectively. This phenomenon can provide researchers a pathway to improve thermal rectification by widely and specifically blocking the phonon modes.

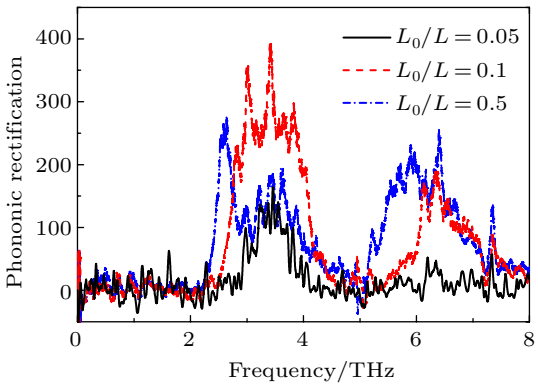

Fig. 4. Length effect on phononic rectification. The phononic rectification efficiency of the phononic rectifier with the sizes of $L_0/L = 0.05$, 0.1, and 0.5. The temperatures are fixed at $T_{\rm hot} = 500$ K and $T_{\rm cold} = 100$ K.

4.3. Temperature effect

The temperature is also a key factor in determining the phononic rectification. Figure 5(a) studies the $L_0/L = 0.05$ system with the cold temperature varying from 30 K to 100 K, meanwhile the hot temperature is fixed at 500 K. Because of the relative weak phonon–phonon scattering strength in HGS at low temperatures, the variation of temperature at the cold side has negligible effect on the phononic rectification. The Lorentzian function fitted results in the insert of Fig. 5(a) show stable peaks, i.e., in frequency and amplitude, with different low temperatures.

On the contrary, the high temperature has significant effect on the phonon excitation of hybridized modes in HGS. Therefore, when varying the temperature of the hot side, the temperature reveals more obvious effects on the phononic rectification. Firstly, the increase of temperature leads to the larger temperature difference between the hot and cold sides, which results in the increase of the rectification efficiency (see Fig. 5(b)). Moreover, the increase in temperature tends to excite the hybridized modes to the high frequency region. The frequency shifting degree of phononic rectification is not so obvious in Fig. 5(b), due to the fixed temperature in $T_{\rm cold}$.

To realize the frequency tuning of the hybridized mode at HGS, we apply a large temperature difference in the study of phononic rectification in the HGS rectifier. However, at the nanoscale, it is difficult to implement in realistic applications. We expect this phononic rectifier to be possible on a large scale to make the large temperature difference. Moreover, we also find the rectification phenomenon at hybridized modes $\omega_{\rm h}$ under small temperature differences, such as $|\Delta T| = 10$ K or

20 K. Because of the reduced shift of ω_h with a small temperature difference, however, tiny rectification efficiency but a wider rectified spectrum is realized.

Lastly, we would like to have a short discussion about the tuning of phononic rectification in this carbon schwarzite host–guest system. As we discussed about the monochromaticity of phononic rectification in Subsection 4.1, the tuning of phononic rectification should be also related to the guest atoms in HGS. The analytical model from Nakayama and Kaneshita[30] showed that the frequency of hybridized modes ω_h is determined by the mass of the guest atoms and the coupling between the guest atoms and cage, in the form of

$$\omega_h \approx \sqrt{\frac{f}{m}}, \tag{5}$$

where f is the second-order force constant between the guest atoms and cage, and m is the mass of the guest atoms. Therefore, the rectification frequency in the phononic rectifier can be tuned by inserting different guest atoms in the carbon schwarzite cage, with which f and m are simultaneously varied.[23,28] Compared to the on-center rattling of guest atoms in the weakly anharmonic system, the multi-potential well system or high temperature effect[24,46,47] would exhibit the off-center rattling dynamics, which possesses stronger anharmonicity. The strong anharmonicity would further destroy the rectification effect by blocking thermal phonons on a wider spectrum.

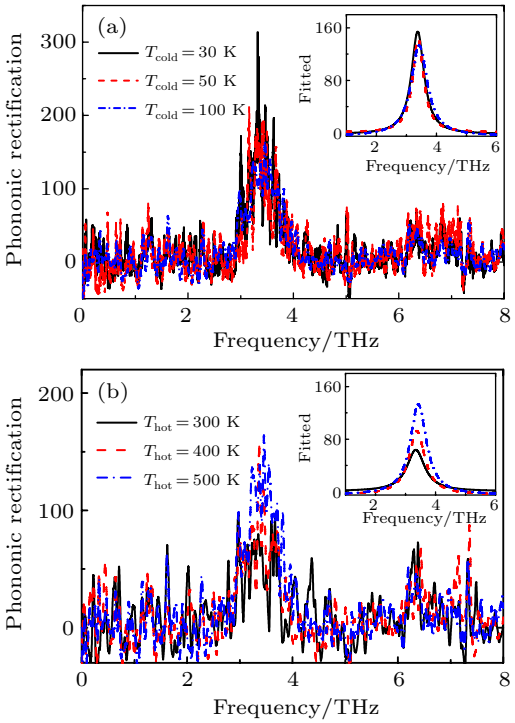

Fig. 5. Temperature effect on phononic rectification. (a) The phononic rectification efficiency of HGS with the cold temperatures T_{cold} = 30 K, 50 K, and 100 K. Here, T_{hot} = 500 K and L_0/L = 0.05. (b) The phononic rectification efficiency of HGS with the hot temperatures T_{hot} = 300 K, 400 K, and 500 K. Here, T_{cold} = 100 K and L_0/L = 0.05. The insert figures in (a) and (b) are the fitted Lorentzian functions for the rectification efficiency spectrum.

5. Conclusion

In this work, by using molecular dynamic simulations, we studied the phononic rectification in a phononic rectifier. The phononic rectifier is constructed based on the carbon schwarzite host–guest system. Compared to the thermal rectification over the full spectrum, our simulations demonstrated that due to the strong confinement of hybridized modes, the phononic rectification in the proposed rectifier only happens at a specific frequency (ω_h). Moreover, the rectification efficiency at ω_h reaches 134%, which is larger than most of the thermal rectification efficiencies in nanostructures. Then, the length and temperature effects on the phononic rectification were discussed. Because of the frequency shift of the hybridized modes in HGS, the increase of the length would block phonons on a broader frequency range, leading to the failure of the rectifier. Besides, the increase of temperature at the hot region also results in the frequency shift of the phononic rectification. Our results propose a new perspective about the thermal phonon rectification, which would be important for controlling monochromatic thermal phonons.

References

[1] Roberts N A and Walker D G 2011 *Int. J. Therm. Sci.* **50** 648
[2] Li N, Ren J, Wang L, Zhang G, Hänggi P and Li B 2012 *Rev. Mod. Phys.* **84** 1045
[3] Zhang Z, Ouyang Y, Cheng Y, Chen J, Li N and Zhang G 2020 *Phys. Rep.* **860** 1
[4] Li B, Wang L and Casati G 2004 *Phys. Rev. Lett.* **93** 184301
[5] Chang C W, Okawa D, Majumdar A and Zettl A 2006 *Science* **314** 1121
[6] Yang N, Zhang G and Li B 2009 *Appl. Phys. Lett.* **95** 033107
[7] Ouyang T, Chen Y, Xie Y, Wei X L, Yang K, Yang P and Zhong J 2010 *Phys. Rev. B* **82** 245403
[8] Ding X and Ming Y 2014 *Chin. Phys. Lett.* **31** 046601
[9] Wang Y, Vallabhaneni A, Hu J, Qiu B, Chen Y P and Ruan X 2014 *Nano Lett.* **14** 592
[10] Chen X K, Xie Z X, Zhou W X, Tang L M and Chen K Q 2016 *Carbon* **100** 492
[11] Zhang Z, Chen Y, Xie Y and Zhang S 2016 *Appl. Therm. Eng.* **102** 1075
[12] Wang H, Hu S, Takahashi K, Zhang X, Takamatsu H and Chen J 2017 *Nat. Commun.* **8** 15843
[13] Hu S, An M, Yang N and Li B 2017 *Small* **13** 1602726
[14] Aiyiti A, Zhang Z, Chen B, Hu S, Chen J, Xu X and Li B 2018 *Carbon* **140** 673
[15] Jiang P, Hu S, Ouyang Y, Ren W, Yu C, Zhang Z and Chen J 2020 *J. Appl. Phys.* **127** 235101
[16] Fugallo G, Cepellotti A, Paulatto L, Lazzeri M, Marzari N and Mauri F 2014 *Nano Lett.* **14** 6109
[17] Zhang Z, Guo Y, Bescond M, Chen J, Nomura M and Volz S 2020 arXiv:2003.02384
[18] Safavi-Naeini A H, Mayer Alegre T P, Chan J, Eichenfield M, Winger M, Lin Q, Hill J T, Chang D E and Painter O 2011 *Nature* **472** 69
[19] Gustafsson M V, Aref T, Kockum A F, Ekström M K, Johansson G and Delsing P 2014 *Science* **346** 207
[20] Cohen J D, Meenehan S M, MacCabe G S, Groblacher S, Safavi-Naeini A H, Marsili F, Shaw M D and Painter O 2015 *Nature* **520** 522
[21] Wang L and Li B 2007 *Phys. Rev. Lett.* **99** 177208
[22] Han H, Li B, Volz S and Kosevich Y A 2015 *Phys. Rev. Lett.* **114** 145501
[23] Zhang Z, Hu S, Xi Q, Nakayama T, Volz S, Chen J and Li B 2020 *Phys. Rev. B* **101** 081402

[24] Takabatake T, Suekuni K, Nakayama T and Kaneshita E 2014 *Rev. Mod. Phys.* **86** 669
[25] Xi Q, Zhang Z, Chen J, Zhou J, Nakayama T and Li B 2017 *Phys. Rev. B* **96** 064306
[26] Xi Q, Zhang Z, Nakayama T, Chen J, Zhou J and Li B 2018 *Phys. Rev. B* **97** 224308
[27] Chen C, Zhang Z and Chen J 2018 *Front. in Ener. Res* **6** 34
[28] Dong J, Sankey O F, Ramachandran G K and McMillan P F 2000 *J. Appl. Phys.* **87** 7726
[29] Zhang Z, Hu S, Nakayama T, Chen J and Li B 2018 *Carbon* **139** 289
[30] Nakayama T and Kaneshita E 2011 *J. Phys. Soc. Jpn.* **80** 104604
[31] Pailhès S, Euchner H, Giordano V M, Debord R, Assy A, Gomes S, Bosak A, Machon D, Paschen S and de Boissieu M 2014 *Phys. Rev. Lett.* **113** 025506
[32] Tagami M, Liang Y, Naito H, Kawazoe Y and Kotani M 2014 *Carbon* **76** 266
[33] Zhang Z, Chen J and Li B 2017 *Nanoscale* **9** 14208
[34] Lherbier A, Terrones H and Charlier J C 2014 *Phys. Rev. B* **90** 125434
[35] O'Keeffe M, Adams G B and Sankey O F 1992 *Phys. Rev. Lett.* **68** 2325
[36] Lindsay L and Broido D A 2010 *Phys. Rev. B* **81** 205441
[37] Rappe A K, Casewit C J, Colwell K S, Goddard W A and Skiff W M 1992 *J. Am. Chem. Soc.* **114** 10024
[38] Hoover W G 1985 *Phys. Rev. A* **31** 1695
[39] Plimpton S 1995 *J. Comput. Phys.* **117** 1
[40] Schelling P K, Phillpot S R and Keblinski P 2002 *Phys. Rev. B* **65** 144306
[41] An M, Li L, Hu S, Ding Z, Yu X, Demir B, Yang N, Ma W and Zhang X 2020 *Carbon* **162** 202
[42] Larkin J M, Turney J E, Massicotte A D, Amon C H and McGaughey A J H 2014 *J. Comput. Theor. Nanosci.* **11** 249
[43] Bao H, Chen J, Gu X and Cao B 2018 *ES Energy Environ.* **1** 16
[44] Sääskilahti K, Oksanen J, Tulkki J and Volz S 2014 *Phys. Rev. B* **90** 134312
[45] Sääskilahti K, Oksanen J, Tulkki J and Volz S 2016 *Phys. Rev. E* **93** 052141
[46] Schopf D, Euchner H and Trebin H R 2014 *Phys. Rev. B* **89** 214306
[47] Tadano T and Tsuneyuki S 2018 *Phys. Rev. Lett.* **120** 105901